applied sciences

MDPI

Article

An Anti-Swing Closed-Loop Control Strategy for Overhead Cranes

Xianghua Ma * and Hanqiu Bao *

School of Electrical and Electronic Engineering, Shanghai Institute of Technology, Shanghai 201418, China
* Correspondence: xhuam@sit.edu.cn (X.M.); 166101105@mail.sit.edu.cn (H.B.)

Received: 13 July 2018; Accepted: 22 August 2018; Published: 25 August 2018

Featured Application: This paper provides a solution to anti-swing control for overhead cranes for outdoor use. This contribution can also be used for other kind of underactuated systems.

Abstract: The payload swing of an overhead crane needs to be controlled properly to improve efficiency and avoid accidents. However, the swing angle is usually very difficult to control to zero degrees or for it to even remain within an acceptable range because the overhead crane is a complex nonlinear underactuated system, especially when the actual working environment is accompanied by strong disturbances and great uncertainty. To resolve this, a real-time anti-swing closed-loop control strategy is proposed that considers external disturbances. The swing angle is measured in time and it functions with the load displacement as feedback inputs of the closed-loop system. The nonlinear model of the crane is simplified by a linear system with virtual disturbances, which are estimated by the equivalent input disturbance (EID) method. Both simulation and experimental results for a 2-D overhead crane system are investigated to illustrate the validity of the proposed method.

Keywords: overhead crane system; anti-swing closed-loop control; swing angle measurement; equivalent input disturbance

1. Introduction

Overhead cranes play an important role as one of the tools of heavy cargo transportation in seaports, steel plants, and other workplaces [1]. As a typical underactuated system, an overhead crane is easily affected by various external disturbances so that the load is frequently swinging in the process of transportation, which seriously affects the positioning accuracy of the load and brings many unsafe possibilities while at the same time of reducing the efficiency of the system [2,3]. Avoiding the swing of the upload and improving safety and efficiency are the main concerns for the study of cranes. Hence, the control objective of an overhead crane generally includes two parts: fast and accurate positioning and effective swing suppression, especially considering external resistance (such as wind resistance, stochastic collision) during the transportation of uploads.

Recently, much research has been done to solve the abovementioned problems. The most common and direct control is input shaping, by which suitable trajectories are planned for the trolley by thoroughly analyzing the coupling between the trolley motion and the payload swing [4–8]. A modified composite nonlinear feedback strategy has been proposed to improve the transient performance and eliminate the steady-state errors in path-following control considering the tire force saturations [9]. To simplify the controller design, partial feedback linearization operations were used in [10–12]. As the solution to the existence of uncertainties in the crane system, an adaptive control method was proposed in [13–15]. In addition, more intelligent methods have been followed to increase the robustness of these methods. A particle swarm optimizer in [16] was applied to determine the optimal sequence of control increments in the presence of constraints on input and output variables. The control scheme was successfully tested on a laboratory-scale overhead crane for different constraints and operating conditions. An error tracking control method was used in [17], for which the error trajectories of the trolley and the payload swing can be prespecified. Some other new complexity control methods have also been put forward to guarantee fast and accurate positioning and effective swing suppression, such as passivity-based control schemes [18–21] and sliding mode control (SMC) methods [22–24]. Regarding unknown inputs, the state and the output vectors of a system can be reconstructed [25]. Also relevant are the complete Lyapunov-based stability analysis in [26], genetic-algorithm-based control [27], and fuzzy logic-based methods [28–30].

However, most of the above methods are based on some harsh assumptions, for example, the initial payload swing angle should be zero, the accurate real-time angle of the payload swing can be known a priori, or velocity sensor measurements can be taken without noise. In fact, the payload easily swings within an unacceptable range in actual working environments, where some external disturbances such as wind resistance and stochastic collision frequently occur. Therefore, these above methods are weak in disturbance suppression and poor for real applications because they belong to open-loop control structures. A closed-loop control system with the feedback of real-time angle measurement values of the payload swing is the most effective way to tackle the anti-swing problem. Further, overhead cranes are usually linearly modeled, which ignores their nonlinear characteristics and thus cannot guarantee a crane's practical performance. Therefore, an anti-swing closed-loop control strategy is proposed in this paper. This control system has two feedback quantities of trolley moving displacement and swing angle, which are both measured in real time. The nonlinear characteristics hidden in the crane system are transformed into an equivalent input disturbance, which can be estimated by a disturbance predictor.

This paper consists of the following four parts: a simplified model of a 2-D overhead crane system is given in Section 2. The controller design is described in detail in Section 3. The control strategy is verified by simulation and experiments in Section 4. The conclusion is presented in Section 5.

2. Mathematical Model

Usually, an overhead crane consists of a hoist, load, and transport trolley, as shown in Figure 1. Its corresponding two-dimensional simplified physical model is shown in Figure 2.

Figure 1. A real crane diagram with hoist and load.

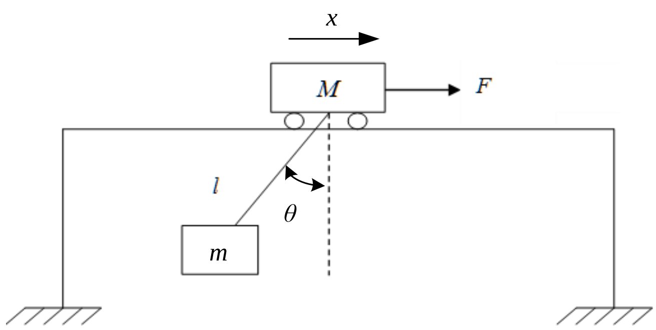

Figure 2. Two-dimensional plane model of an overhead crane.

Assuming that the length of hoisting rope l does not change during transportation and the friction between the trolley and the platform μ is negligible, that is $\dot{l} = \ddot{l} = 0,\ \mu = 0$, the dynamic equation of the 2-D overhead crane system is obtained as follows:

$$\begin{bmatrix} ml^2 & ml\cos\theta \\ ml\cos\theta & M+m \end{bmatrix}\begin{bmatrix} \ddot{\theta} \\ \ddot{x} \end{bmatrix} + \begin{bmatrix} 0 & 0 \\ -ml\dot{\theta}\sin\theta & 0 \end{bmatrix}\begin{bmatrix} \dot{\theta} \\ \dot{x} \end{bmatrix} + \begin{bmatrix} mgl\sin\theta \\ 0 \end{bmatrix} = \begin{bmatrix} 0 \\ F(t) \end{bmatrix} \tag{1}$$

where M, m is the mass of the trolley and the hoist, respectively, $x(t)$ is the horizontal displacement, $\theta(t)$ is the vertical direction angle of the upload, and $F(t)$ is the driving force. $M(x,\ \theta) = \begin{bmatrix} m_{11} & m_{12} \\ m_{21} & m_{22} \end{bmatrix} = \begin{bmatrix} ml^2 & ml\cos\theta \\ ml\cos\theta & M+m \end{bmatrix}$ is the inertial matrix of the system (1).

Known from [31], although a 2-D underactuated system cannot be fully state-feedback linearized, $\ddot{x}$ can be implemented as a system input, and the driven state quantity part $[x, \dot{x}]$ can be linearized. Inspired by this, the model of the 2-D overhead crane can be transformed by homeomorphism coordinate transformation:

$$\Gamma\begin{cases} z_1 = x + \alpha(\theta) \\ z_2 = \dfrac{\partial L(x,\ \theta)}{\partial \dot{x}} = m_{11}\dot{x} + m_{12}\dot{x} \\ z_3 = \theta \\ z_4 = \dot{\theta} \end{cases} \tag{2}$$

where $L(x, \theta)$ is the Lagrange equation of the 2-D overhead crane system.

Simultaneously from (1), (2) is obtained:

$$\dot{z} = f(z) + Bu \tag{3}$$

where:

$$\begin{aligned} & f_1(z) = [\frac{z_2}{m_{11}} + (\frac{d\alpha(\theta)}{d\theta} - \frac{m_{11}}{m_{12}})z_4]\Big|_{\zeta=\Gamma^{-1}(z)} \\ & f_2(z) = [\frac{1}{2}[\dot{x}, \dot{\theta}]^{\mathrm{T}}\frac{\partial M(x,\theta)}{\partial x} - mgl\sin\theta]\Big|_{\zeta=\Gamma^{-1}(z)} \\ & f(z) = [f_1(z), f_2(z), z_4, 0]^{\mathrm{T}} \\ & B = [0,0,0,1]^{\mathrm{T}} \\ & \zeta = [x, \theta, \dot{x}, \dot{\theta}]^{\mathrm{T}} \end{aligned}$$

The value of the costate coefficient $\alpha(\theta)$ is set 0 in this paper to ensure the conciseness of the transformed system structure. It is proved later that the controllability and observability of the system is not affected by the choice of the value of $\alpha(\theta)$.

Define:

$$\sigma = f(z) - Az \tag{4}$$

The system (1) is equivalent to the following mathematical model:

$$\begin{cases} \dot{z} = Az + Bu + \sigma \\ y = Cz \end{cases} \tag{5}$$

where:

$$A = \frac{\partial f(z)}{\partial z}|_{z=0} = \begin{bmatrix} a_{11} & a_{12} & a_{13} & a_{14} \\ a_{21} & a_{22} & a_{23} & a_{24} \\ 0 & 0 & 0 & 1 \\ 0 & 0 & 0 & 0 \end{bmatrix},\ a_{ij} = \frac{\partial f_i(z)}{\partial z_j}|_{z=0},\ i = 1,2,\ j = 1,2,3,4$$
$$C = \begin{bmatrix} 1 & 0 & 0 & 0 \\ 0 & 0 & 1 & 0 \end{bmatrix}$$

From mathematical description (8), a conclusion can be made that the nonlinear crane system (1) can be equivalent to a linear combination of a linear subsystem and a nonlinear term. The nonlinear term σ can be treated as a virtual disturbance. For the linear subsystem, it can be controlled and observed if and only if the following inequality is satisfied:

$$\left[\frac{m_{12}}{m_{11}}\frac{\partial(mgl\sin\theta)}{\partial x} - \frac{\partial(mgl\sin\theta)}{\partial\theta}\right]|_{x,\theta=0} \neq 0,\ -\frac{1}{m_{11}\ (x=0)} < 0 \tag{6}$$

3. Controller Design and Analysis

A dual-loop feedback control system was proposed to realize the swing attenuation of the payload. The swing angle and displacement were measured in real time and were used as a feedback into the model predictive controller (MPC), as illustrated in the block diagram of the proposed control system in Figure 3. The MPC method was adopted to find future control input changes to reduce errors caused by the load swings. The desired swing angle with reference trajectories was also the input of the controller. A disturbance predictor was used to estimate the real-time value of the equivalent input disturbance σ_e.

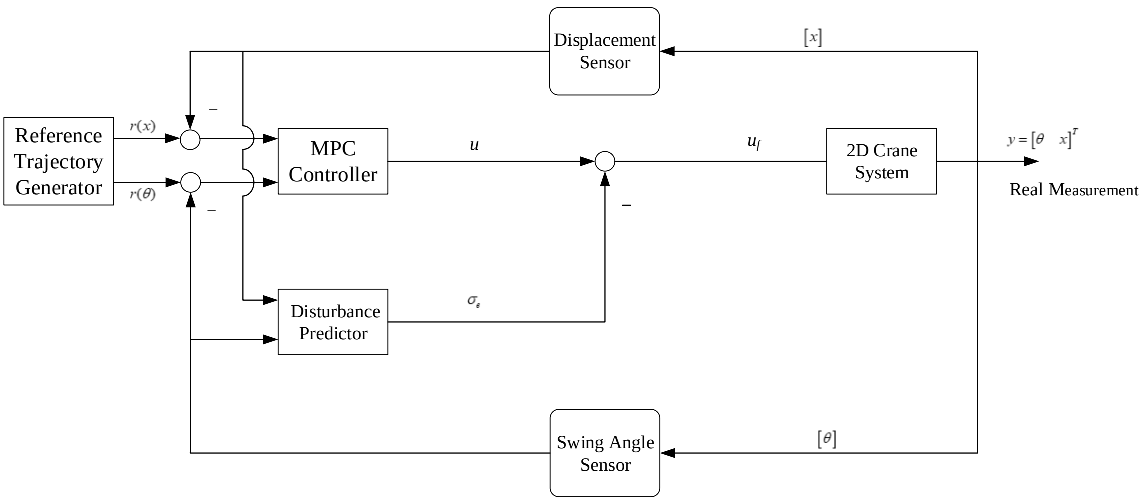

Figure 3. The block diagram of the proposed closed-loop control system.

(1) Estimation of Equivalent Input Disturbances

$$\dot{\hat{z}} = A\hat{z} + Bu_f + L(y - C\hat{z}) \tag{7}$$

L is the observer gain. Define $\Delta z = \hat{z} - z$, σ = B σ_e, we have

$$\dot{\hat{z}} = A\hat{z} + Bu + B\sigma_e + (\Delta\dot{z} - A\Delta z) \tag{8}$$

Suppose there exists a $\Delta\sigma$ satisfying

$$\Delta\dot{z} - A\Delta z = B\Delta\sigma \tag{9}$$

Combine (8) and (9):

$$\dot{\hat{z}} = A\hat{z} + B(u_f + \hat{\sigma}_e) \tag{10}$$

where $\hat{\sigma}_e = \sigma_e + \Delta\sigma$, combine (8) with (10):

$$B(u + \hat{\sigma}_e - u_f) = L(y - C\hat{z}) \tag{11}$$

At the same time on both sides, multiply by B^{T}:

$$\hat{\sigma}_e = B^{+}L(y - C\hat{z}) + u - u_f \tag{12}$$

Take the value of $\hat{\sigma}_e$ as the predicted value of the equivalent input disturbance σ_e, where $B^{+} = \left(B^T B\right)^{-1} B^T$. In addition, in order to ensure the accuracy of the equivalent input disturbance prediction, we introduced a low-pass filter $F(s)$ to adjust the predicted frequency segment:

$$F(s) = \frac{1}{Ts + 1} \tag{13}$$

where T is a time constant.

(2) Control Algorithm

The sampling period was selected as T_m, and the linear part system can be discretized as follows:

$$\begin{cases} z_m(k+1) = A_p z_m(k) + B_p u(k) \\ y(k) = C_p z_m(k) \end{cases}, C_p = I_{4\times 4} \tag{14}$$

where $z_m(k)$ and $y(k)$ denote the system state and the output at time k, respectively, and $A_p \in \mathrm{R}^{4\times 4}$, $B_p \in \mathrm{R}^{4\times 1}$ represent the discrete system parameter matrices. $\mathrm{I}_{4\times 4} \in \mathrm{R}^{4\times 4}$ is the 4×4 identity matrix, which can be calculated as

$$A_P = \exp(AT_m), B_P = A^{-1}\,(A_P - I_{4\times 4})B$$

where $\exp(*)$ represents the natural exponential function. Next, we proposed a proper MPC formula to control this discrete system (14).

For the crane system, our purpose was to transport the payload to the desired position without residual oscillation, with the desired transportation distance defined as x_d, while the target of the output vector $y(k)$ was defined as

$$y_f = \begin{bmatrix} x_d & 0 & 0 & 0 \end{bmatrix}^{\mathrm{T}}$$

To calculate the optimal input, a cost function is defined as

$$J(k_i) = \|w_p(k_i) - y(k_i)\|_Q^2 + \|\Delta u(k_i)\|_R^2 \tag{15}$$

where Q, R are the error weight matrix and control weight matrix, respectively, and $w_P(k_i)$ is the reference output value, which are defined as

$$
\begin{aligned}
w_P(k_i) &= \begin{bmatrix} w(k_i+1) & w(k_i+2) & \cdots & w(k_i+P) \end{bmatrix}^{\mathrm{T}} \\
Q &= diag\begin{pmatrix} q_1 & \cdots & q_P \end{pmatrix} \\
R &= diag\begin{pmatrix} r_1 & \cdots & r_P \end{pmatrix}
\end{aligned}
$$

At each sampling time, the trolley needs to track a proper trajectory to reach the target position. The reference trajectory with the soften factor is designed as follows:

$$r(\bullet) = w_p(k) = f(y(k-1), y_f) \tag{16}$$

4. Simulation and Experiment

Simulations in the environment of MATLAB/Simulink and experiments based on a laboratory-scale overhead crane were implemented to validate the performance of the proposed control strategy as shown in Figure 4. As for the simulation, a Luenberger full-dimensional state observer was used to estimate the real-time swing angle.

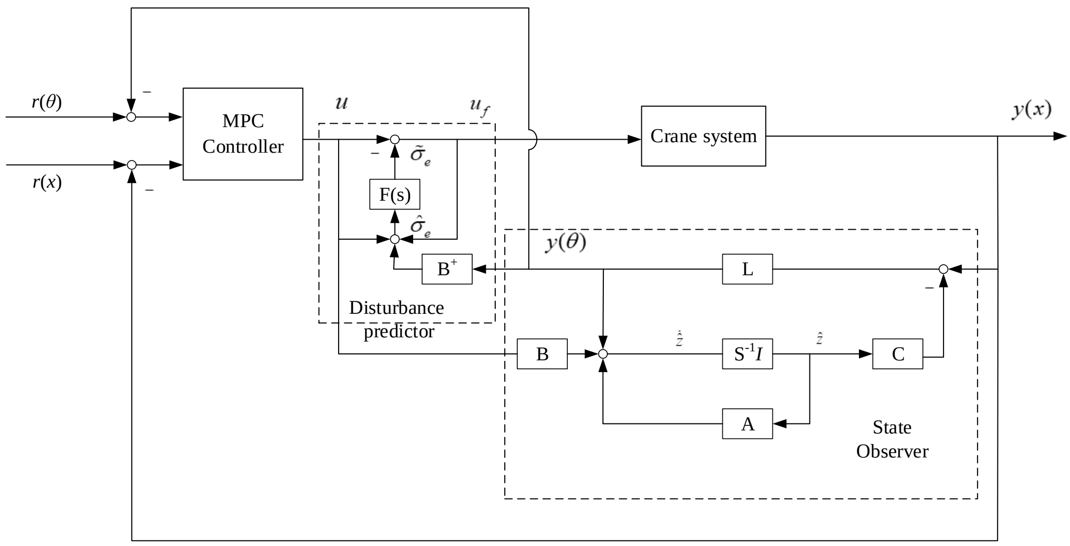

Figure 4. The simulation structure of the proposed anti-swing closed-loop control system.

(1) Simulation

The simulation parameters of the overhead crane were as follows: m = 50 kg, l =3 m and M = 70 kg, g = 9.8 m/s^2. The control strategy was validated under the different conditions of expected horizontal move distance x_d and expected arriving time t_f.

Simulation 1. *Expected horizontal move distance and expected time was* x_d *= 5 m,* t_f *= 30 s.*

Simulation 2. *Expected horizontal move distance and expected time was* x_d *= 10 m,* t_f *= 30 s.*

Simulation 3. *Expected horizontal move distance and expected time was* x_d *= 10 m,* t_f *= 30 s.*

During the transportation process, a duration of 1 s of white noise disturbance was added at t_1 *= 5 s,* t_2 *= 15 s, and* t_3 *= 25 s.*

Simulation 4. *Expected horizontal move distance and expected time was* x_d *= 10 m,* t_f *= 30 s.Since Proportion Integration Differentiation (PID) and its improved algorithm currently are the main approach to solve the swing problem, the method proposed in this article (abbreviated as MPC-EID) was also compared with the classical double-closed-loop PID (abbreviated as DPID) and fuzzy-PID (abbreviated as FPID). We also compared our* *method with the method that adopts an internal model with the equivalent input disturbance (abbreviated as IEID) control algorithm, which is the same idea in the model establishment of the underactuated system.*

It can be seen from Figures 5 and 6 that when the crane is moving horizontally, the swing angle is always within 1 degree, and the swing angle has almost decreased to 0 degrees when the crane reaches the target location within the expected time t_f. The entire control process is more natural and smooth.

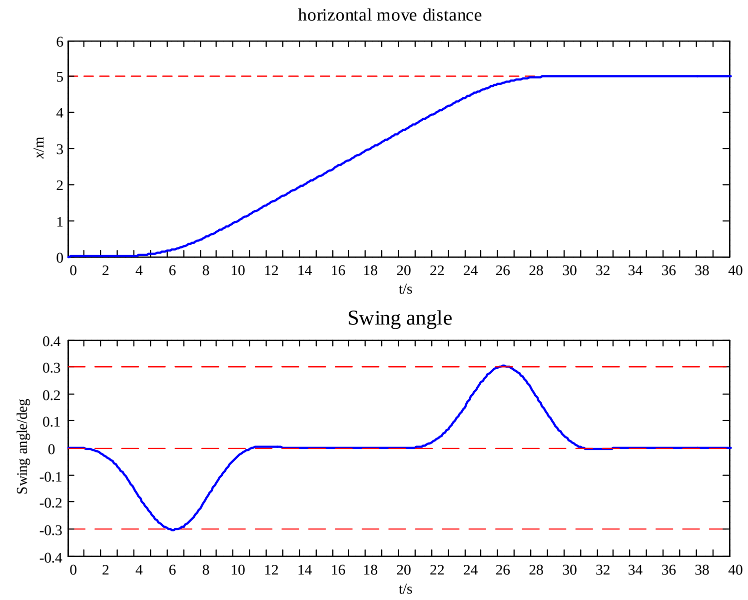

Figure 5. Result of simulation 1.

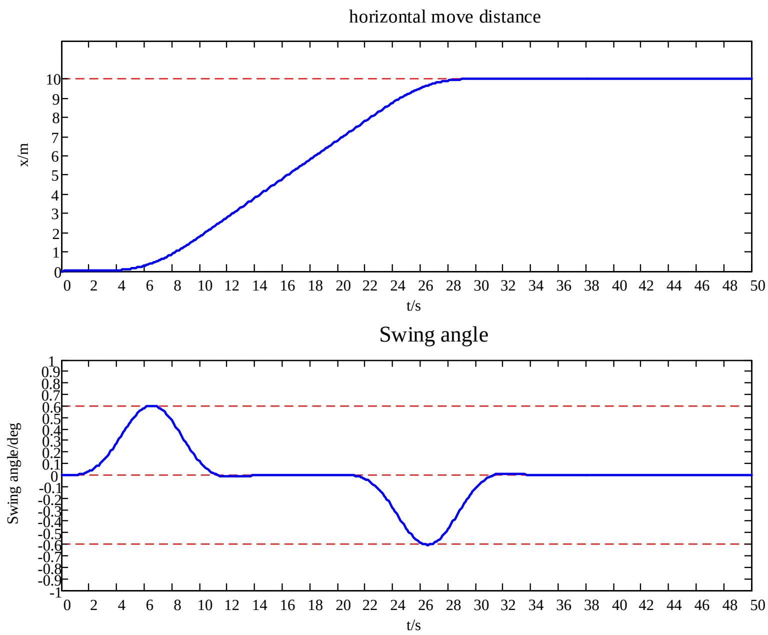

Figure 6. Result of simulation 2.

From Figure 7, the swing angle has some fluctuations when 1 s of white noise disturbance is added to the control system, but it can quickly return to the normal swing within a certain period of time.

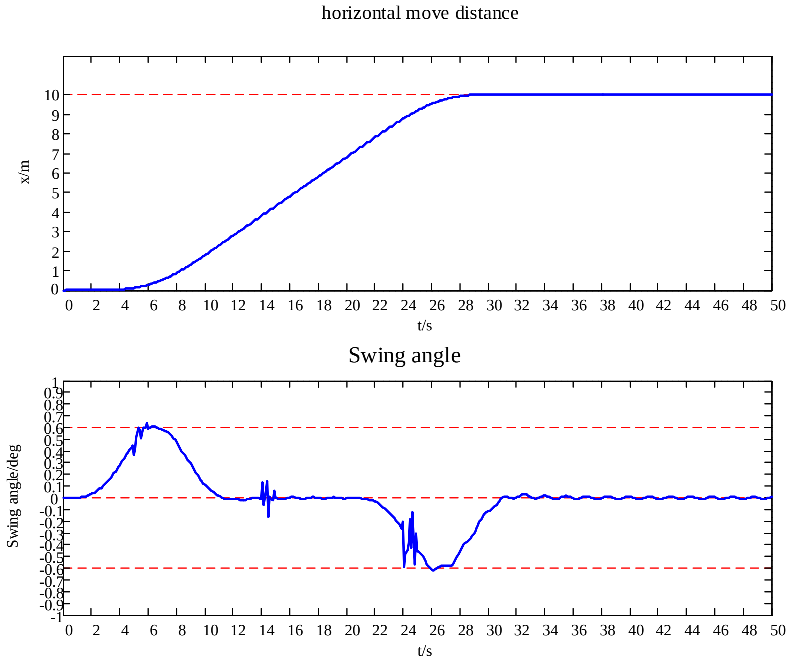

Figure 7. Result of simulation 3.

From the simulation results of the four kinds of methods in Figure 8, we can see that the FPID and DPID methods have quite similar results. As for the time taken to arrive at the target location, the least time is taken by the FPID and DPID methods and the most time by the IEID method. As for the time for the swing angle value to reach zero degrees, the FPID and DPID methods both take about 30 s (the DPID method actually goes a little bit faster than the FPID method), the IEID method takes 35 s, and the MPC-EID method takes 31 s. However, the maximum swing angle by the DPID method can reach more than 0.6 degrees, and the minimum swing angle by the IEID method can reach 0.5 degrees. The MPC-EID method has moderate performance, which is the relatively best solution for safety and efficiency in real applications.

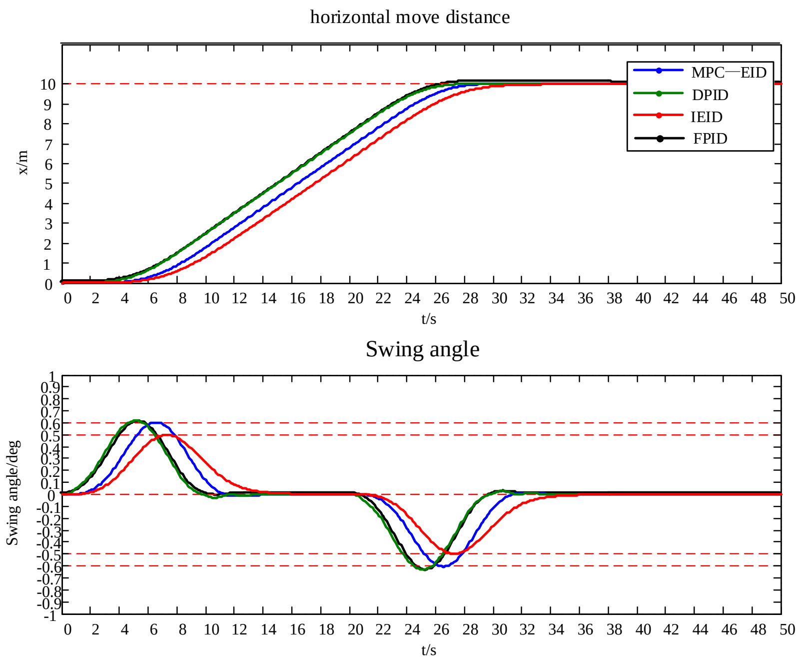

Figure 8. Result of simulation 4.

(2) Experiments

A lab was specially built to validate the proposed method, as shown in Figure 9. The experimental platform used three Alternating Current (AC) asynchronous motors to drive the trolley to move on the track. The maximum speed was 1 m/s. Due to the limitation of the experimental site, the track length of the crane was 5.5 m, the actual usable length was 5 m, and the maximum rope length was 3 m. The maximum payload mass was 1 t. The moving distance sensor used in this experiment could achieve an accuracy of 1 mm. Using the aircraft attitude angle sensor, the dynamic swing angle and the static swing angle accuracy could reach 0.01°. The friction coefficient was 0.2. The swing angle of the payload was required to remain within ±50 mm after the mechanism stopped in 5 s.

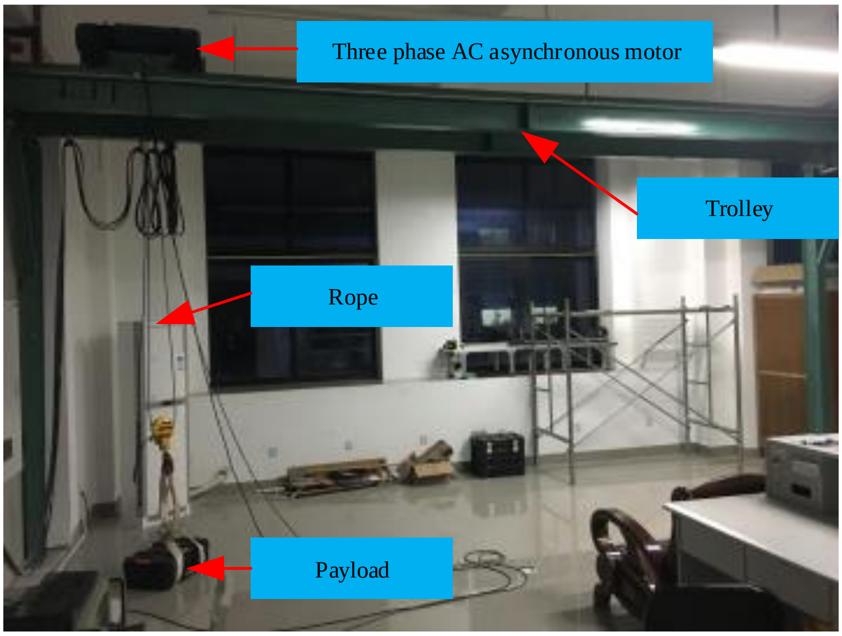

Figure 9. Main mechanical structure of the laboratory-scale overhead crane.

Experiment 1. *Expected horizontal move distance and expected time was* x_d = *3.83 m,* t_f = *15 s. The MPC-EID method proposed in this article) was also compared with the FPID method.*

Experiment 2. *Expected horizontal move distance and expected time was* x_d = *3.83 m,* t_f = *15 s. In* t_{s1} = *4 s,* t_{s2} = *9 s, and* t_{s3} = *14 s, an external disturbance was exerted.*

We can see that the experimental results in Figure 10 show some obvious differences. Although the maximum swing angle controlled by the FPID method was 0.2 degrees, much larger than that by the MPC-EID method, the swing angle by the FPID method converged faster than that of the MPC-EID method. However, the swing angle fluctuation by the FPID method was also larger than that by the MPC-EID method when the swing angle was controlled within a certain range. We can conclude that the overhead crane can be controlled more smoothly and safely by the FPID method.

Though the payload was oscillating near zero degrees for about 15 s, as shown in Figure 11, the swing angle was small within an accepted range when the trolley arrived at the designated position. There was also a certain error and delay of the swing angle during the process of transportation because there were a number of noises in the measurement values of the swing angles. The two problems can be solved if a better data processing method is used. This means that the method proposed in this paper can effectively realize the anti-rolling control of the crane when external disturbances exist.

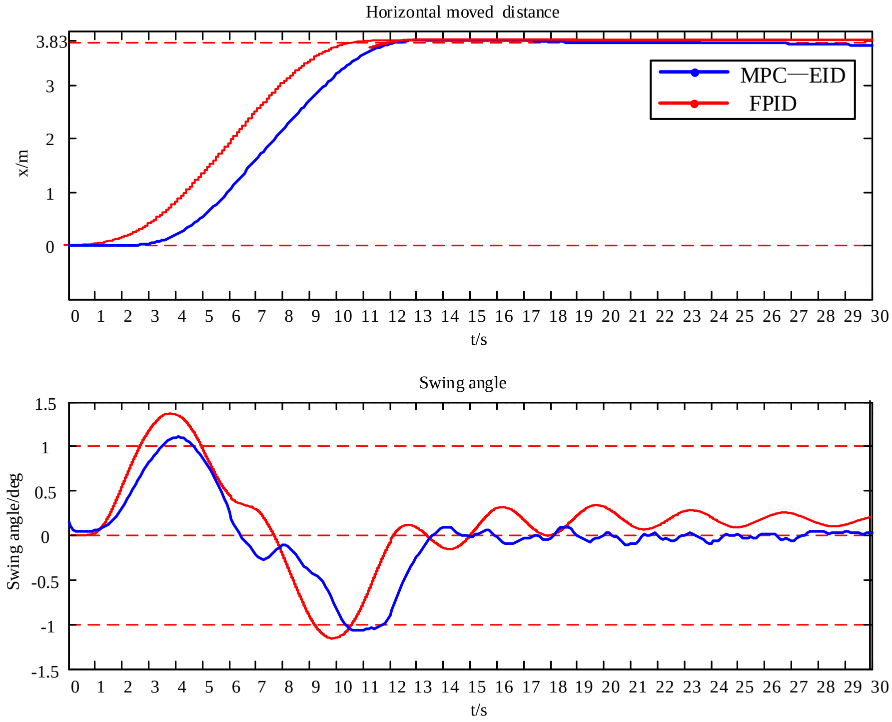

Figure 10. Result of experiment 1.

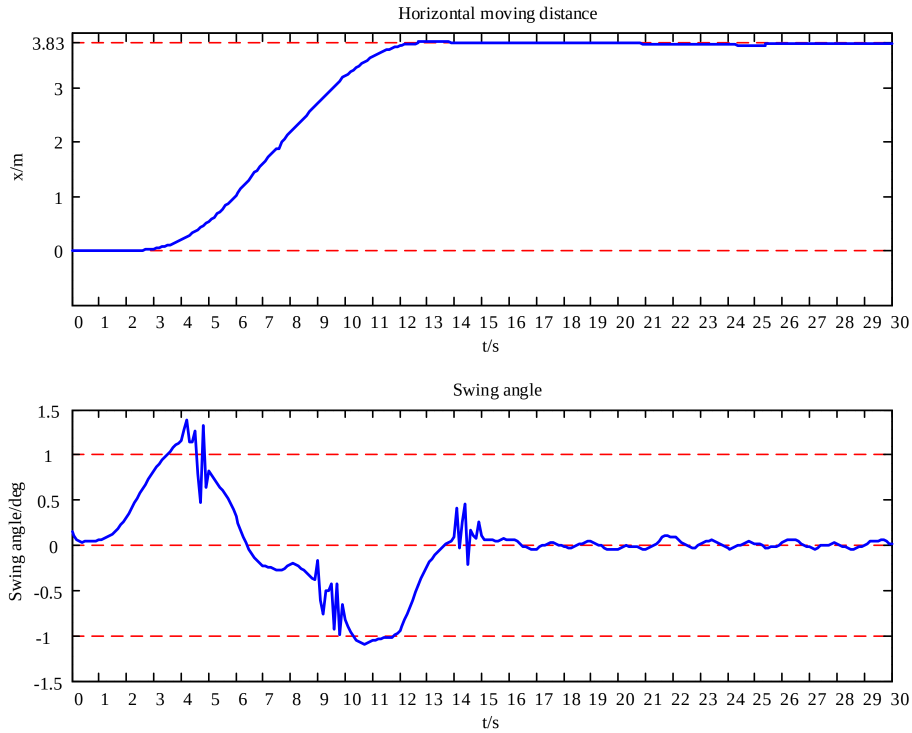

Figure 11. Result of experiment 2.

5. Conclusion

An anti-swing closed-loop control strategy is proposed in this paper to achieve a robust disturbance rejection for underactuated crane systems with two-degree freedom. The proposed method was validated by simulation and experiment. The simulation and experimental results both illustrate the satisfactory performance of the proposed strategy. The swing angle can be controlled within the acceptable range and the external disturbances on the overhead crane system can be successfully suppressed. Our future work will focus on extending the proposed method to a 3-D overhead crane and will consider the hoisting and lowering of the payload during the transportation.

Author Contributions: X.M. and H.B. conceived and designed the experiments; X.M. performed the experiments; X.M. and H.B. analyzed the data; H.B. contributed reagents/materials/analysis tools; X.M. Writing-Original Draft Preparation; X.M. and H.B. Writing-Review & Editing.

Funding: This research was partially funded by National Science Foundation of China [No. 51876089].

Conflicts of Interest: The authors declare no conflict of interest.

References

1. Ramli, L.; Mohamed, Z.; Abdullahi, A.M.; Jaafar, H.I.; Lazim, I.M. Control strategies for crane systems: A comprehensive review. *J. Mech. Syst. Signal Proc.* **2017**, *99*, 1–23. [CrossRef]
2. Colombo, L.; Jiménez, F.; Diego, D.M.D. Variational integrators for underactuated mechanical control systems with symmetries. *J. Comput. Dyn.* **2017**, *2*, 193–225. [CrossRef]
3. Pucci, D.; Romano, F.; Nori, F. Collocated Adaptive Control of Underactuated Mechanical Systems. *IEEE Trans. Rob.* **2017**, *31*, 1527–1536. [CrossRef]
4. Maghsoudi, M.J.; Mohamed, Z.; Sudin, S.; Buyamin, S.; Jaafar, H.I.; Ahmad, S.M. An improved input shaping design for an efficient sway control of a nonlinear 3D overhead crane with friction. *J. Mech. Syst. Signal Proc.* **2017**, *92*, 364–378. [CrossRef]
5. Smoczek, J.; Szpytko, J. Comparision of model predictive, input shaping and feedback control for a lab-scaled overhead crane. In Proceedings of the 2016 21st International Conference on Methods and Models in Automation and Robotics (MMAR), Miedzyzdroje, Poland, 29 August–1 September 2016.
6. Kjelland, M.B.; Hansen, M.R. Using input shaping and pressure feedback to suppress oscillations in slewing motion of lightweight flexible hydraulic crane. *Int. J. Fluid Power* **2015**, *16*, 141–148. [CrossRef]
7. Majid, M.A.; Wan, W.S.; Mohamad, S.; Bakar, Z.A. A comparison of PID and PD controller with input shaping technique for 3D gantry crane. In Proceedings of the IEEE Conference on Systems, Process & Control (ICSPC), Kuala Lumpur, Malaysia, 13–15 December 2013.
8. Hu, Y.; Wu, B.; Vaughan, J.; Singhose, W. Oscillation suppressing for an energy efficient bridge crane using input shaping. In Proceedings of the 2013 9th Asian Control Conference, Istanbul, Turkey, 23–26 June 2013.
9. Hu, C.; Wang, R.; Yan, F.; Chadli, M.; Karimi, H.R. Composite Nonlinear Feedback Control for Path Following of Four-Wheel Independently Actuated Autonomous Ground Vehicles. *IEEE Trans. Intell. Transp. Syst.* **2016**, *17*, 2063–2074.
10. Lee, S.G.; Le, A.T.; Moon, S.C. Partial Feedback Linearization and Sliding Mode Techniques for 2D Crane Contro. *Trans. Inst. Meas. Control* **2014**, *36*, 78–87. [CrossRef]
11. Hilhorst, G.; Pipeleers, G.; Michiels, W.; Oliveira, R.C.L.F.; Peres, P.L.D.; Swevers, J. Fixed-Order Linear Parameter-Varying Feedback Control of a Lab-Scale Overhead Crane. *IEEE Trans. Control Syst. Technol.* **2016**, *24*, 1899–1907. [CrossRef]
12. Dong, H.Q.; Lee, S.G.; Ba, P.D. Double-loop control with proportional-integral and partial feedback linearization for a 3D gantry crane. In Proceedings of the 17th International Conference on Control, Automation and Systems (ICCAS), Ramada Plaza, Jeju, Korea, 18–21 October 2017.
13. Sun, N.; Fang, Y.; Chen, H.; He, B. Adaptive Nonlinear Crane Control With Load Hoisting/Lowering and Unknown Parameters: Design and Experiments. *IEEE/ASME Trans. Mechatron.* **2015**, *20*, 2107–2119. [CrossRef]
14. Qian, Y.; Fang, Y.; Lu, B. Adaptive repetitive learning control for an offshore boom crane. *Automatica* **2017**, *82*, 21–28. [CrossRef]
15. Zhang, M.; Ma, X.; Rong, X.; Song, R.; Tian, X.; Li, Y. A partially saturated adaptive learning controller for overhead cranes with payload hoisting/lowering and unknown parameters. *Nonlinear Dyn.* **2017**, *89*, 1779–1791. [CrossRef]
16. Smoczek, J.; Szpytko, J. Particle Swarm Optimization-Based Multivariable Generalized Predictive Control for an Overhead Crane. *IEEE/ASME Trans. Mech.* **2017**, *22*, 258–268. [CrossRef]

17. Zhang, M.; Ma, X.; Rong, X.; Tian, X.; Li, Y. Error tracking control for underactuated overhead cranes against arbitrary initial payload swing angles. *Mech. Sys. Signal Proc.* **2017**, *84*, 268–285. [CrossRef]
18. Wu, X.; He, X. Nonlinear Energy-Based Regulation Control of Three-Dimensional Overhead Cranes. *IEEE Trans. Autom. Sci. Eng.* **2017**, *14*, 1297–1308. [CrossRef]
19. Zhan, Y.; Wu, X.; He, X. Control of the double-container overhead crane. In Proceedings of the 2015 34th Chinese Control Conference, Hangzhou, China, 28–30 July 2015.
20. Hoang, N.Q.; Lee, S.G.; Kim, H.; Moon, S.C. Trajectory planning for overhead crane by trolley acceleration shaping. *J. Mech. Sci. Technol.* **2014**, *28*, 2879–2888. [CrossRef]
21. Kazi, F.; Banavar, R.N.; Mullhaupt, P.; Bonvin, D. Stabilization of a 2D-SpiderCrane Mechanism Using Damping Assignment Passivity-based Control. *IFAC Proc. Vol.* **2008**, *41*, 3155–3160. [CrossRef]
22. Ngo, Q.H.; Nguyen, N.P.; Nguyen, C.N.; Tran, T.H.; Ha, Q.P. Fuzzy sliding mode control of an offshore container crane. *Ocean Eng.* **2017**, *140*, 125–134. [CrossRef]
23. Chwa, D. Sliding Mode Control-based Robust Finite-Time Anti-Sway Tracking Control of 3-D Overhead Cranes. *IEEE Trans. Ind. Electron.* **2017**, *64*, 6775–6784. [CrossRef]
24. Lu, B.; Fang, Y.; Sun, N. Sliding mode control for underactuated overhead cranes suffering from both matched and unmatched disturbances. *Mechatronic* **2017**, *47*, 116–125. [CrossRef]
25. Akhenak, A.; Chadli, M.; Maquin, D.; Ragot, J. Sliding mode multiple observer for fault detection and isolation. In Proceedings of the 42nd IEEE Conference on Decision Control, Maui, HI, USA, 9–12 December 2003.
26. Sun, N.; Wu, Y.; Fang, Y.; Chen, H. Nonlinear antiswing control for crane systems with double-pendulum swing effects and uncertain parameters: design and experiments. *IEEE Trans. Autom. Sci. Eng.* **2017**, *15*, 1–10. [CrossRef]
27. Al-Dhaheri, N.; Jebali, A.; Diabat, A. A simulation-based Genetic Algorithm approach for the quay crane scheduling under uncertainty. *Simul. Model. Pract. Theory* **2016**, *66*, 122–138. [CrossRef]
28. Qian, D.; Tong, S.; Lee, S.G. Fuzzy-Logic-based control of payloads subjected to double-pendulum motion in overhead cranes. *Autom. Constr.* **2016**, *65*, 133–143. [CrossRef]
29. Rong, B.; Rui, X.; Tao, L.; Wang, G. Dynamics analysis and fuzzy anti-swing control design of overhead crane system based on Riccati discrete time transfer matrix method. *Multibody Sys. Dyn.* **2018**, *43*, 279–295. [CrossRef]
30. Yang, T.; Qiu, W.; Ma, Y.; Chadli, M.; Zhang, L.X. Fuzzy model-based predictive control of dissolved oxygen in activated sludge processes. *Neurocomputing* **2014**, *136*, 88–95. [CrossRef]
31. Spong, M. The swing up control problem for the acrobot. *IEEE Control Sys.* **1995**, *15*, 49–55.